Figure4:Hsp32-targeting drugs synergize with bendamustine and with BCR/ABL1-targeting drugs in producing growth inhibition and apoptosis in ALL cells. A: The Ph+ ALL cell line TOM-1 was incubated in control medium or various concentrations of imatinib and SMA-ZnPP or a combination of both drugs for 48h. Thereafter, ³H-thymidine incorporation was measured. Results represent the mean±S.D. of triplicate experiments and are expressed in percent of control. B,C: The Ph+ ALL cell line Z-119 was incubated with control medium or various concentrations of imatinib, nilotinib, PEG-ZnPP, or SMA-ZnPP, alone or with a combination (with fixed drug ratio) of these drugs as indicated for 24 hours. Thereafter, the percentages of apoptotic cells were determined by light microscopy. Results represent the mean±S.D. of three independent experiments. D: The ALL cell lines NALM-1 and TOM-1 were left untransfected (Co) or were transfected with a control siRNA against luciferase (Luc siRNA) or siRNA against Hsp32 (200 nM each) as described in the text. 48 hours after transfection, cells were incubated in control medium or various concentrations of imatinib for 48h. Thereafter, ³H-thymidine incorporation was measured. Results represent the mean±S.D. of triplicate experiments and are expressed as percent of control.

DISCUSSION

Recent data suggest that Hsp32 is an important survival factor and potential target in various malignant cells [22-27]. We have recently shown that CML cells constitutively express Hsp32 and that the disease-related oncoprotein BCR/ABL1 promotes expression of Hsp32 in Ba/F3 cells [28,29]. In the present study, we show that Hsp32 is also expressed and serves as an essential 'survival-molecule' in Ph+ and Ph− ALL cells. Our data also show that Hsp32-targeting drugs induce apoptosis and growth arrest in ALL cells and synergize with BCR/ABL1 TKI and with bendamustin in producing growth inhibition in imatinib-sensitive and imatinib-resistant ALL cells. Together, these data suggest that Hsp32 is a potential new target in ALL.

Expression of Hsp32 in ALL cells was demonstrable by qPCR and Western blotting as well as by immunocytochemistry. Interestingly, both the Ph+ ALL cells and Ph− ALL cells were found to express Hsp32, suggesting that apart from BCR/ABL1, other mechanisms and molecules may also contribute to expression of this 'survival-molecule' in leukemic cells. Baseline levels of Hsp32 were comparable in Ph+ and Ph− ALL cells and were upregulated by hemin.

In Ph+ CML, BCR/ABL1 promotes the expression of Hsp32 in leukemic cells [28]. To explore the potential role of this pathway in expression of Hsp32 in Ph+ ALL cells, we treated these cells with BCR/ABL1-targeting drugs. We found that BCR/ABL1 TKI downregulate the expression of Hsp32 mRNA in Ph+ ALL cells. These data suggest that BCR/ABL1 may contribute to expression of Hsp32 in Ph+ ALL cells. However, as mentioned, Hsp32 was also detectable in Ph− ALL cells. From these data, we hypothesize that expression of Hsp32 can also be triggered by other pathways in ALL cells. Indeed it has been described that several different oncoproteins, including JAK2 V617F, KIT D816V or RAS G12V induce expression of Hsp32/HO-1 in neoplastic cells [30]. The exact nature of additional HO-1-promoting oncogenic lesions in ALL cells remains at present unknown. Alternatively, Hsp32 expression in ALL cells may also be regulated by external factors. In this regard it is noteworthy that Hsp32 is an established "stress-induced" survival factor in various physiologic cells and that several different stimuli, including chemotherapy agents, can induce expression of Hsp32/HO-1 in malignant cells [30].

To demonstrate that Hsp32 serves as a survival factor in ALL cells, we performed experiments using ALL cell lines and siRNA against Hsp32. The observation that the siRNA-induced knock-down is associated with apoptosis and growth arrest in these cells suggests that Hsp32 serves as an important survival factor in ALL cells and thus may represent a potential therapeutic target.

In the past few years, two water-soluble pharmacologic inhibitors of Hsp32, SMA-ZnPP and PEG-ZnPP, have been developed and tested in experimental solid tumors [22-27]. In the current study these two inhibitors were applied to target Hsp32 in ALL cells. Both inhibitors were found to downregulate growth and survival in primary (Ph+ and Ph−) ALL cells as well as in all ALL cell lines tested. By contrast, the Hsp32 inhibitors showed no major effects on viability of normal cells [28]. All in all, these data suggest that pharmacologic targeting of Hsp32 in ALL cells may result in their selective apoptosis and growth arrest.

A major clinical challenge in the treatment of ALL is resistance to imatinib and other BCR/ABL1 TKI [10-13]. Therefore, a number of novel agents and pharmacologic approaches are currently under investigation, with the aim to overcome drug-resistance. In the present study, we found that PEG-ZnPP and SMA-ZnPP induce growth arrest and apoptosis not only in imatinib-sensitive ALL cells but also in imatinib-resistant cells, which may be of clinical interest. These data are also in line with our previous observations that Hsp32 inhibitors block the growth of imatinib-resistant CML cells as well as Ba/F3 cells expressing various imatinib-resistant mutants of BCR/ABL1, including the T315I mutant that renders BCR/ABL1 resistant against all currently available BCR/ABL1 TKI [29]. In the present study, we examined one CML patient in lymphoid blast phase exhibiting the T315I mutant. As expected, both PEG-ZnPP and SMA-ZnPP were found to suppress the growth of leukemic cells in this patient. Together, our data suggest that targeting of Hsp32 may be an interesting approach to treat patients with drug-resistant Ph+ ALL or lymphoid blast phase of CML.

An attractive strategy to overcome drug resistance in leukemias is to combine various targeted drugs with each other or with conventional drugs. The data of our study show that Hsp32-targeting drugs synergize with imatinib and with nilotinib as well as with bendamustine in producing growth inhibition in Ph+ and Ph− ALL cells. These synergistic drug effects were seen in imatinib-sensitive as well as in imatinib-resistant ALL cells, supporting the notion that Hsp32 may be an attractive new therapeutic target in this disease. This hypothesis was further supported by the observation that siRNA against HO-1 substantially augments the growth-inhibitory effects of imatinib on ALL cells.

In summary, our data show that Hsp32 is an important survival factor and potential new target in leukemic cells in Ph+ and Ph− ALL, including patients with TKI-resistant disease. Clinical studies are now warranted to show whether targeting of Hsp32 alone or in combination with BCR/ABL1 TKI or other inhibitors, can induce clinically relevant responses in patients.

MATERIALS AND METHODS

Reagents

Pegylated zinc protoporphyrin (PEG-ZnPP) and ZnPP encapsulated in the micelle of styrene maleic acid (SMA-ZnPP), were produced as described previously [31-33]. Imatinib and nilotinib (AMN107) were kindly provided by Dr.E.Buchdunger and Dr.P.W.Manley (Novartis Pharma AG, Basel, Switzerland). Bendamustine was kindly provided by Dr.D.Guggi (Mundipharma, Vienna, Austria). RPMI 1640 medium and fetal calf serum (FCS) were purchased from PAA laboratories (Pasching, Austria), hemin and bovine serum albumin (BSA) from Sigma-Aldrich (St. Louis, Mo), and lipofectin from Invitrogen (Carlsbad, CA).

Primary ALL cells and cell lines

For *in vitro* culture experiments, primary leukemic cells were obtained from 11 patients with Ph$^+$ ALL, 15 with Ph$^-$ ALL, 4 with T-ALL, 2 with biphenotypic acute leukemia, and one with a lymphoid blast phase of CML with *BCR/ABL1* T315I. For polymerase chain reaction (PCR) analysis, frozen samples from 10 patients with Ph$^+$ ALL and 10 with Ph$^-$ ALL were used. In 8 patients (5 with Ph+ ALL and 3 with Ph- ALL), CD34$^+$/CD38$^-$ cells and CD34$^+$/CD38$^+$ cells were purified by cell sorting (purity >98%) as described [34]. The patients´ characteristics are shown in Table 1. Written informed consent was obtained in each case. The study was approved by the Ethics Committee of the Medical University of Vienna, Austria. The following Ph$^+$ ALL cell lines were used: Z-119, BV-173, TOM-1, and NALM-1. In addition, a number of Ph$^-$ lymphatic cell lines were used: Raji, Ramos, REH, and BL-41. Z-119 cells were kindly provided to J.V.M. by Dr. Zeev Estrov (MD Anderson Cancer Centre, Houston, Texas, USA). All other cell lines were purchased from the Leibnitz Institute DSMZ-German Collection of Microorganisms and Cell Cultures (Braunschweig, Germany). The identity of the cell lines was reconfirmed by DNA sequencing and DNA profiling (by nonaplex PCR) and by studying the presence or absence of *BCR/ABL1*. Cell lines were cultured in RPMI 1640 medium and 20% heat-inactivated FCS at 37°C and 5% CO_2. Table 2 shows a summary of characteristics of cell lines tested in this study.

Real time PCR

RNA was isolated from primary ALL cells and cell lines using the RNeasy MinEluteCleanupKit (Qiagen, Hiden, Germany). cDNA was synthesized using Moloney murine leukemia virus reverse transcriptase (Invitrogen), random primers, First Strand buffer, dNTPs (100 mM), and RNasin (all from Invitrogen) according to the manufacturer`s instructions. PCR was performed using primers specific for Hsp32 and ABL: Hsp32: 5´-CAGGATTTGTCAGAGGCC CTGAAGG-3´ (forward), 5´-TGTGGTACAGGGAGGCCATCACC-3´ (reverse); ABL: 5´-TGTATGATTTTGTGGCCAGTGGAG-3´ (forward), and 5´-GCCTA AGACCCGGAGCTTTTCA-3´ (reverse). mRNA levels were quantified on a 7900HT Fast Real-Time PCR System (Applied Biosystem, Foster City, CA) using iTAq SYBR Green Supermix with ROX (Bio-Rad, Hercules, CA). Hsp32 mRNA expression levels were normalized to ABL mRNA levels. Calculations were based on standard curves established for Hsp32 and ABL mRNA expression. Hsp32 mRNA levels were expressed as percentage of ABL mRNA.

Immunocytochemistry

Immunocytochemistry was performed on cytospin-slides prepared with primary neoplastic cells, sorted ALL stem cells, and cell lines. A polyclonal rabbit anti- HO-1 (anti-Hsp32) antibody (Stressgen, Ann Arbor, MI; dilution 1:100) and a biotinylated goat-anti-rabbit IgG (Biocare, San Diego, CA) were applied essentially as described [28,35]. Slides were incubated with the primary antibody overnight, washed, and were then incubated with second-step antibody for 30 minutes. Streptavidin-alkaline-phosphatase complex (Biocare) was used as chromogen. Antibody reactivity was made visible using Neofuchsin (Nichirei, Tokyo, Japan). Slides were counterstained in Mayer`s hemalaun. In control experiments, the primary antibody was preincubated with control buffer or a Hsp32-specific blocking peptide (Stressgen) before being applied.

Western blotting

The Ph$^+$ cell line Z-119 and the Ph$^-$ cell line BL-41 were incubated with hemin (10 μM, 37°C, 8 hours) before being analyzed. Western blotting was performed using a polyclonal rabbit anti-Hsp32 antibody (Stressgen) and an anti--actin antibody (Santa Cruz), as described [28,35]. Antibody reactivity was made visible by donkey anti-rabbit IgG antibody and Lumigen PS-3 detection reagent (both from GE Healthcare, Buckinghamshire, UK).

Design and application of siRNA against Hsp32

siRNA against Hsp32 (5'-AAGCUUUCUGGUGGCGACAGUdTdT-3') as well as a control siRNA against luciferase (5'-CUUACGCUGAGUACUUCG AdTdT-3') were

synthesized by Dharmacon Research (Lafayette, CO). The siRNA (200 nM) was transfected into NALM-1, Raji and TOM-1, using lipofectin (Invitrogen) as reported [35]. Proliferation of transfected and control cells was analyzed by determining ^{3}H-thyimidine uptake. In addition, the percentage of apoptotic cells was determined by Wright-Giemsa staining after 48 hours. In a separate set of experiments, siRNA-transfected NALM-1 and TOM-1 cells were incubated in various concentrations of imatinib (10-24 nM) at 37°C for 48 hours. Then, cells were examined for proliferation by measuring ^{3}H-thyimidine uptake.

Proliferation assay

To examine anti-proliferative effects of PEG-ZnPP and SMA-ZnPP, Ph$^+$ and Ph$^-$ ALL cell lines and primary ALL cells were cultured in 96-well microtiter plates (5 x 10^4 cells per well) in the absence or presence of various concentrations of PEG-ZnPP or SMA-ZnPP for 48 hours, followed by addition of ^{3}H-thymidine (0.5 μCi per well) for 16 hours. Cells were harvested on filter membranes (Packard Bioscience, Meriden, CT) in a Filtermate 96 harvester (Packard Bioscience). Filters were air-dried, and the bound radioactivity was measured in a -counter (Top-Count NXT, Packard Bioscience). All experiments were performed in triplicate. In a separate set of experiments, cell lines were cultured in the presence of various drug combinations at a fixed concentration-ratio for each combination: PEG-ZnPP+imatinib, PEG-ZnPP+nilotinib, PEG-ZnPP+bendamustine, SMA-ZnPP+imatinib, SMA-ZnPP+nilotinib, and SMA-ZnPP+bendamustine.

Apoptosis assays

The effects of SMA-ZnPP and PEG-ZnPP on cell viability (apoptosis) were analyzed by morphologic examination. Cells were incubated with various concentrations of SMA-ZnPP or PEG-ZnPP (1-20 μM) at 37°C for 48 hours. The percentage of apoptotic cells was quantified on Wright-Giemsa-stained cytospin slides [36]. In select experiments, Hsp32-targeting drugs were applied in combination with TKI (imatinib or nilotinib) or bendamustine. To confirm apoptosis in drug-exposed cells, combined AnnexinV/propidium-iodide staining was performed using the apoptosis detection kit from Alexis Biochemicals (Lausen, Switzerland) as described [29]. Cells were analyzed by flow cytometry on a FACScan (Becton Dickinson, San Jose, CA). A Tunel assay was performed using the 'In situ cell death detection kit' (Roche, Mannheim, Germany) as reported [35]. In brief, cells were incubated with 10 μM SMA-ZnPP, 5 μM PEG-ZnPP, or control medium for 48 hours and then spun on cytospin slides, fixed in 4% paraformaldehyde, washed, and permeabilized in 0.1% Triton X-100 and 0.1 % sodium citrate. Then, cells were washed and incubated in terminal-transferase reaction-solution for 60 minutes at 37°C. Cells were analyzed under a Carl Zeiss Imager. A1 microscope (Carl Zeiss, Jena, Germany). For caspase 3 detection, cell lines were incubated in control medium or in various concentrations of SMA-ZnPP (5-20 μM) at 37°C for 48 hours. Then, cells were fixed in 2% formaldehyde (room temperature, 10 minutes), permeabilized in 100% methanol at -20°C (15 minutes), washed in PBS plus BSA (0.1%), and then stained with the FITC-conjugated mAb C92-605 (Becton Dickinson Biosciences) directed against active caspase 3 for 1 hour. Thereafter, cells were analyzed by flow cytometry on a FACSCalibur (Becton Dickinson Biosciences).

Statistical analysis

The paired Student´s t test was applied in growth inhibition-experiments. Results were considered to be significantly different, when the p-value was <0.05. Drug combination effects (additive versus synergistic) were determined by calculating the combination index (CI) values using Calcusyn software (Calcusyn; Biosoft, Ferguson, MO) [37]. A CI value of 1 indicates additive effects and a CI below 1 indicates synergistic drug interactions.

REFERENCES

1. Faderl S, Jeha S, Kantarjian HM. The biology and therapy of adult acute lymphoblastic leukemia. Cancer. 2003;98:1337-1354.

2. Armstrong SA, Look AT. Molecular genetics of acute lymphoblastic leukemia, J Clin Oncol. 2005;23:6306-6315.

3. Pui CH, Robison LL, Look AT. Acute lymphoblastic leukaemia. Lancet. 2008;371:1030-1043.

4. Crazzolara R, Bendall L. Emerging treatments in acute lymphoblastic leukemia. Curr Cancer Drug Targets. 2009;9:19-31.

5. Faderl S, Kantarjian HM, Talpaz M, Estrov Z. Clinical significance of cytogenetic abnormalities in adult acute lymphoblastic leukemia. Blood. 1998;91:3995-4019.

6. Gleissner B, Gökbuget N, Bartram CR, Janssen B, Rieder H, Janssen JW, Fonatsch C, Heyll A, Voliotis D, Beck J, Lipp T, Munzert G, Maurer J, et al. Leading prognostic relevance of the BCR-ABL translocation in adult acute B-lineage lymphoblastic leukemia: A prospective study of the German Multicenter Trial Group and confirmed polymerase chain reaction analysis. Blood. 2002;99:1536-

1543.

7. Druker BJ, Sawyers CL, Kantarjian H, Resta DJ, Reese SF, Ford JM, Capdeville R. Activity of a specific inhibitor of the BCR-ABL tyrosine kinase in the blast crisis of chronic myeloid leukemia and acute lymphoblastic leukemia with the Philadelphia chromosome. N Engl J Med. 2001;344:1038-1042.

8. Ottmann OG, Druker BJ, Sawyers CL, Goldman JM, Reiffers J, Silver RT, Tura S, Fischer T, Deininger MW, Schiffer CA, Baccarani M, Gratwohl A, Hochhaus A, et al. A phase 2 study of imatinib in patients with relapsed or refractory Philadelphia chromosome-positive acute lymphoid leukemias. Blood. 2002;100:1965-1971.

9. Thomas DA, Faderl S, Cortes J, O'Brien S, Giles FJ, Kornblau SM, Garcia-Manero G, Keating MJ, Andreeff M, Jeha S, Beran M, Verstovsek S, Pierce S, et al. Treatment of Philadelphia chromosome–positive acute lymphocytic leukemia with hyper-CVAD and imatinib mesylate. Blood. 2004;103:4396–4407.

10. Towatari M, Yanada M, Usui N, Takeuchi J, Sugiura I, Takeuchi M, Yagasaki F, Kawai Y, Miyawaki S, Ohtake S, Jinnai I, Matsuo K, Naoe T, et al. Japan Adult Leukemia Study Group. Combination of intensive chemotherapy and imatinib can rapidly induce high-quality complete remission for a majority of patients with newly diagnosed BCR-ABL–positive acute lymphoblastic. Blood. 2004;104:3507–3512.

11. Yanada M, Takeuchi J, Sugiura I, Akiyama H, Usui N, Yagasaki F, Kobayashi T, Ueda Y, Takeuchi M, Miyawaki S, Maruta A, Emi N, Miyazaki Y, et al. High complete remission rate and promising outcome by combination of imatinib and chemotherapy for newly diagnosed BCR-ABL-positive acute lymphoblastic leukemia: a phase II study by the Japan Adult Leukemia Study Group. J Clin Oncol. 2006;24:460–466.

12. Hölzer D, Gökbuget N, Ottmann OG. Targeted therapies in the treatment of Philadelphia chromosome-positive acute lymphoblastic leukemia. Semin Hematol. 2002;39:32-37.

13. Vitale A, Guarini A, Chiaretti S, Foà R. The changing scene of adult acute lymphoblastic leukemia. Curr Opin Oncol. 2006;18:652-659.

14. Liu-Dumlao T, Kantarjian H, Thomas DA, O'Brien S, Ravandi F. Philadelphia-positive acute lymphoblastic leukemia: current treatment options. Curr Oncol Rep. 2012;14:387-394.

15. Chao NJ, Blume KG, Forman SJ, Snyder DS. Long-term follow-up of allogeneic bone marrow recipients for Philadelphia chromosome-positive acute lymphoblastic leukemia. Blood. 1995;85:3353-3354.

16. Fielding AK, Goldstone AH. Allogeneic haematopoietic stem cell transplant in Philadelphia-positive acute lymphoblastic leukaemia. Bone Marrow Transplant. 2008;41:447-453.

17. Lee S, Kim YJ, Min CK, Kim HJ, Eom KS, Kim DW, Lee JW, Min WS, Kim CC. The effect of first-line imatinib interim therapy on the outcome of allogeneic stem cell transplantation in adults with newly diagnosed Philadelphia chromosome-positive acute lymphoblastic leukemia. Blood. 2005;105:3449-3457.

18. Stein A, Forman SJ. Allogeneic transplantation for ALL in adults. Bone Marrow Transplant. 2008;41:439-446.

19. Jego G, Hazoumé A, Seigneuric R, Garrido C. Targeting heat shock proteins in cancer. Cancer Lett. 2013;332:275-285.

20. Morse D, Choi AM. Heme oxygenase-1: the "emerging molecule" has arrived. Am J Respir Cell Mol Biol. 2002;27:8-16.

21. Ryter SW, Otterbein LE, Morse D, Choi AM. Heme oxygenase/carbon monoxide signaling pathways: regulation and functional significance. Mol Cell Biochem. 2002;234-5:249-263.

22. Fang J, Akaike T, Maeda H. Antiapoptotic role of heme oxygenase (HO) and the potential of HO as a target in anticancer treatment. Apoptosis. 2004;9:27-35.

23. Doi K, Akaike T, Fujii S, Tanaka S, Ikebe N, Beppu T, Shibahara S, Ogawa M, Maeda H. Induction of haem oxygenase-1 nitric oxide and ischaemia in experimental solid tumours and implications for tumour growth. Br J Cancer. 1999;80:1945-1954.

24. Fang J, Sawa T, Akaike T, Akuta T, Sahoo SK, Khaled G, Hamada A, Maeda H. In vivo antitumor activity of pegylated zinc protoporphyrin: targeted inhibition of heme oxygenase in solid tumor. Cancer Res. 2003;63:3567-3574.

25. Liu ZM, Chen GG, Ng EK, Leung WK, Sung JJ, Chung SC. Upregulation of heme oxygenase-1 and p21 confers resistance to apoptosis in human gastric cancer cells. Oncogene. 2004;23:503-513.

26. Berberat PO, Dambrauskas Z, Gulbinas A, Giese T, Giese N, Künzli B, Autschbach F, Meuer S, Büchler MW, Friess H. Inhibition of heme oxygenase-1 increases responsiveness of pancreatic cancer cells to anticancer treatment. Clin Cancer Res. 2005;11:3790-3798.

27. Was H, Cichon T, Smolarczyk R, Rudnicka D, Stopa M, Chevalier C, Leger JJ, Lackowska B, Grochot A, Bojkowska K, Ratajska A, Kieda C, Szala S, et al. Overexpression of heme oxygenase-1 in murine melanoma: increased proliferation and viability of tumor cells, decreased survival of mice. Am J Pathol. 2006;169:2181-2198.

28. Mayerhofer M, Florian S, Krauth MT, Aichberger KJ, Bilban M, Marculescu R, Printz D, Fritsch G, Wagner O, Selzer E, Sperr WR, Valent P. Identification of heme oxygenase-1 as a novel BCR/ABL-dependent survival factor in chronic myeloid leukemia. Cancer Res. 2004;64:3148-154.

29. Mayerhofer M, Gleixner KV, Mayerhofer J, Hoermann G, Jaeger E, Aichberger KJ, Ott RG, Greish K, Nakamura H, Derdak S, Samorapoompichit P, Pickl WF, Sexl V, et al. Targeting of heat shock protein 32 (Hsp32)/heme

oxygenase-1 (HO-1) in leukemic cells in chronic myeloid leukemia: a novel approach to overcome resistance against imatinib. Blood. 2008;111:2200-2210.

30. Gleixner KV, Mayerhofer M, Vales A, Gruze A, Hörmann G, Cerny-Reiterer S, Lackner E, Hadzijusufovic E, Herrmann H, Iyer AK, Krauth MT, Pickl WF, Marian B, et al. Targeting of Hsp32 in solid tumors and leukemias: a novel approach to optimize anticancer therapy. Curr Cancer Drug Targets. 2009;9:675-689.

31. Sahoo SK, Sawa T, Fang J, Tanaka S, Miyamoto Y, Akaike T, Maeda H. Pegylated zinc protoporphyrin: a water-soluble heme oxygenase inhibitor with tumor-targeting capacity. Bioconjug Chem. 2002;13:1031-1038.

32. Fang J, Sawa T, Akaike T, Akuta T, Sahoo SK, Khaled G, Hamada A, Maeda H. In vivo antitumor activity of pegylated zinc protoporphyrin: targeted inhibition of heme oxygenase in solid tumor. Cancer Res. 2003;63:3567-3574.

33. Iyer AK, Greish K, Fang J, Murakami R, Maeda H. High-loading nanosized micelles of copoly(styrene-maleic acid)-zinc protoporphyrin for targeted delivery of a potent heme oxygenase inhibitor. Biomaterials. 2007;28:1871-1881.

34. Herrmann H, Cerny-Reiterer S, Gleixner KV, Blatt K, Herndlhofer S, Rabitsch W, Jäger E, Mitterbauer-Hohendanner G, Streubel B, Selzer E, Schwarzinger I, Sperr WR, Valent P. CD34+/CD38- stem cells in chronic myeloid leukemia express Siglec-3 (CD33) and are responsive to the CD33-targeting drug gemtuzumab/ozogamicin. Haematologica. 2012;97:219-226.

35. Kondo R, Gleixner KV, Mayerhofer M, Vales A, Gruze A, Samorapoompichit P, Greish K, Krauth MT, Aichberger KJ, Pickl WF, Esterbauer H, Sillaber C, Maeda H, et al. Identification of heat shock protein 32 (Hsp32) as a novel survival factor and therapeutic target in neoplastic mast cells. Blood. 2007;110:661-669.

36. Van Cruchten S, Van Den Broeck W. Morphological and biochemical aspects of apoptosis, oncosis and necrosis. Anat Histol Embryol. 2002;31:214-223.

37. Chou TC, Talalay P. Quantitative analysis of dose-effect relationships: the combined effects of multiple drugs or enzyme inhibitors. Adv Enzyme Regul. 1984;22:27-55.
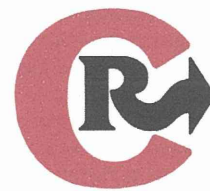
Styrene-maleic acid copolymer-encapsulated CORM2, a water-soluble carbon monoxide (CO) donor with a constant CO-releasing property, exhibits therapeutic potential for inflammatory bowel disease

Q1 Hongzhuan Yin [a,1,2], Jun Fang [a,b,*,2], Long Liao [a,c], Hideaki Nakamura [a,c], Hiroshi Maeda [a,**]

[a] DDS Research Institute, Sojo University, Ikeda 4-22-1, Nishi-ku, Kumamoto 860-0082, Japan
[b] Laboratory of Microbiology and Oncology, Faculty of Pharmaceutical Sciences, Sojo University, Ikeda 4-22-1, Nishi-ku, Kumamoto 860-0082, Japan
[c] Department of Applied Microbial Technology, Faculty of Biotechnology and Life Science, Sojo University, Ikeda 4-22-1, Nishi-ku, Kumamoto 860-0082, Japan

ABSTRACT

Carbon monoxide (CO), the physiological product of heme oxygenase during catabolic breakdown of heme, has versatile functions and fulfills major anti-oxidative and anti-apoptotic roles in cell systems. Administration of CO is thus thought to be a reasonable therapeutic approach in diseases—such as inflammatory bowel disease—that are induced by reactive oxygen species (ROS). Tricarbonyldichlororuthenium(II) dimer (CORM2) is a commonly used CO donor, but it has poor aqueous solubility and a very short CO-releasing half-life ($t_{1/2}$). In the present study, we prepared micelles consisting of water-soluble styrene-maleic acid copolymer (SMA) encapsulating CORM2 (SMA/CORM2) that had a hydrodynamic size of 165.3 nm. Compared with free CORM2, SMA/CORM2 demonstrated better water solubility (>50 mg/ml in a physiological water solution). Moreover, because of micelle formation in an aqueous environment, the CO release rate was slow and sustained. These properties resulted in much longer in vivo bioactivity of SMA/CORM2 compared with that of free CORM2, i.e. the $t_{1/2}$ in blood of SMA/CORM2 in mice after intravenous (i.v.) injection was about 35 times longer than that of free CORM2. We then evaluated the therapeutic potential of SMA/CORM2 in a murine model of inflammatory colitis induced by dextran sulfate sodium (DSS). Administration (either i.v. or oral) of SMA/CORM2 once at the beginning of colitis, 3 days after DSS treatment, significantly improved colitis symptoms—loss of body weight, diarrhea, and hematochezia—as well as histopathological colonic changes—shortening of the colon and necrosis or ulcers in the colonic mucosa. Up-regulation of inflammatory cytokines including monocyte chemotactic protein-1, tumor necrosis factor-α, and interleukin-6 in this DSS-induced colitis was significantly suppressed in SMA/CORM2-treated mice. SMA/CORM2 may thus be a superior CO donor and may be a candidate drug, which involves cytokine suppression, for ROS-related diseases including inflammatory bowel disease.

© 2014 Published by Elsevier B.V.

1. Introduction

For a long time, carbon monoxide (CO) has been best known for its potent toxic effect as an air pollutant, because it has a strong affinity, more than 210-fold greater than that of oxygen, for hemoglobin and thus forms carboxyhemoglobin. More recently, CO was found to behave as an important endogenous signaling molecule in vivo, with versatile biological functions, which include anti-oxidation; regulation of vascular tonus, anti-apoptosis, and anti-inflammatory functions; and induction of angiogenesis [1,2]. In biological systems, which serve as the major source of CO, more than 80% of CO is derived from heme oxygenase (HO) during heme catabolism. Some CO may be produced through photo-oxidation; auto-oxidation of organic molecules, phenols, and flavonoids; and peroxidation of lipids; however, this CO is the consequence of severe stress and may not be observed under physiological conditions [2,3].

HO is the key enzyme in heme degradation, which generates biliverdin, CO, and free iron (Fe^{2+}) [4]. To date, two major HO isoforms have been identified: the constitutive form (HO-2) and the inducible form (HO-1) [4–6]. HO-1, which is now known to be a member of the heat shock protein family, Hsp32, is induced by various stresses and is believed to have fundamental adaptive and defensive functions against various oxidative and cellular stresses [4–6]. Therefore, induction of HO-1 is becoming an effective therapeutic strategy for many diseases including inflammatory diseases related to reactive oxygen species (ROS) [4,5,7]. The anti-oxidative and anti-apoptotic effects of HO are due mostly to the products of heme catabolism: for example, bilirubin, which is

converted from biliverdin by biliverdin reductase, is a potent antioxidant with anti-apoptotic effects under physiological conditions [6,8]. CO has recently attracted increasing attention because of its versatile functions and is believed to account for the major biological properties of HO, if not all of them, and perhaps its therapeutic potential. Accordingly, CO gas and CO donors, as exogenous CO sources, have been developed and utilized as therapeutic agents for ROS-related and other inflammatory diseases [1,2]. The use of CO donors is a more direct and accurate way to evaluate and fulfill the effect of CO and it is easy to control compared to the method of inducing HO-1, in which many mechanisms besides CO production is involved and the induction process may be affected by many *in vivo* conditions such as oxidative and cellular stresses.

The CO-releasing molecule tricarbonyldichlororuthenium(II) dimer (CORM2) has been widely used as a CO donor in various *in vitro* studies, and its *in vivo* application was also reported in a rat liver ischemia-reperfusion model and in a murine colitis model, although its therapeutic effect was less significant [9,10]. However, two major problems remain for CORM2, *i.e.* poor water solubility and short *in vivo* $t_{1/2}$ [11], which greatly hinder its development as a therapeutic agent. To overcome these drawbacks, in this study we designed and prepared a polymer complex of CORM2 by using a biocompatible polymer, styrene-maleic acid copolymer (SMA), aiming at highly water-soluble micelles of CORM2 (SMA/CORM2) with a relatively constant and slow CO release rate. Besides the high water solubility, SMA/CORM2 micelles should have a significantly prolonged circulation time and selective targeting to inflammatory lesions because they take advantage of the enhanced permeability and retention (EPR) effect [12–15]. We thus expected SMA/CORM2 to be beneficial in therapy for ROS-related inflammatory diseases.

Inflammatory bowel disease (IBD) comprises two chronic diseases that cause intestinal inflammation: ulcerative colitis and Crohn's disease [16,17]. Although the exact cause of IBD is unclear, the primary causes are thought to be dysfunctional immunoregulation, genetic disposition, and bacterial infection [16–19]. Moreover, IBD lesions reportedly demonstrated abnormally high levels of ROS, which damage DNA, proteins, and lipids because of extreme reactivity and result in cell death and the initiation and propagation of IBD, which suggests that ROS are involved in the etiology of IBD [20,21]. The use of antioxidant and anti-inflammatory agents may thus help in the treatment of IBD. Indeed, many researchers found antioxidant treatment of IBD to be effective in both animal experiments and clinical settings [10,19–21].

To investigate the therapeutic potential of SMA/CORM2 in IBD, we utilized a dextran sulfate sodium (DSS)-induced colitis model that is characterized by bloody diarrhea, ulceration, and excessive infiltration of inflammatory leukocytes into the colon. We also investigated CO release profiles and the pharmacokinetics of SMA/CORM2 *in vivo* in this model, as well as the effect of SMA/CORM2 on inflammatory cytokines during development of this disease.

2. Materials and methods

2.1. Chemicals

DSS with a mean molecular weight of about 40,000 was purchased from Wako Pure Chemical Co. (Osaka, Japan). 1-Hydroxy-2-oxo-3-(*N*-methyl-3-aminopropyl)-3-methyl-1-triazene (NOC7) was purchased from Dojindo Chemical Laboratories (Kumamoto, Japan). CORM2, lecithin, and saponin were from Sigma-Aldrich (St. Louis, MO, USA). All other chemicals and reagents were from commercial sources unless otherwise described.

2.2. Preparation of SMA/CORM2 micelles

2.2.1. Hydrolysis of SMA

SMA copolymer with a mean molecular weight of 1280 (Mw/Mn: 1.1) was obtained from Kuraray Co. Ltd., Kurashiki, Japan. The maleic anhydride residue of the SMA polymer was hydrolyzed to the water-soluble maleic acid form by dissolving it in 0.1 N NaOH with stirring and heating at 40 °C until a clear solution was obtained after more than 24 h. Then, the hydrolysate was neutralized to pH 7.0 with 0.1 M HCl, followed by dialysis and freeze-drying.

2.2.2. Preparation of SMA/CORM2

We prepared SMA/CORM2 micelles by using our earlier-described method for preparation of SMA/zinc protoporphyrin [22] with some modifications. Briefly, hydrolyzed SMA was dissolved in deionized water at a concentration of 10 mg/ml, and the pH was adjusted to 7.4 with 0.1 N HCl. To this solution we added CORM2 dissolved in dimethyl sulfoxide (DMSO) at a concentration of 20 mg/ml, *via* dropwise addition at the weight ratio of 1:5 (CORM2/SMA). After addition of CORM2, the pH of the reaction mixture was adjusted to 7.2–7.4 by using 0.1 N NaOH, with stirring continued for 2 h at room temperature. The hydrolyzed SMA spontaneously formed micelles by hydrophobic or other non-covalent interactions with CORM2. The resultant SMA/CORM2 micelles were purified by means of dialysis against deionized water, performed three times at 4 °C, with a membrane cutoff Mw of 8000; they were then lyophilized, which yielded weak yellow powder.

2.3. Characterization of SMA/CORM2 micelles

2.3.1. Dynamic light scattering and zeta potential

SMA/CORM2 was dissolved in 0.01 M phosphate-buffered 0.15 M saline (PBS; pH 7.4) at 1 mg/ml and was filtered through a 0.45-µm filter attached to a syringe. The particle size and surface charge (zeta potential) were measured by using a light-scattering instrument (ELS-Z2; Otsuka Electronics Co. Ltd., Osaka, Japan).

2.3.2. Transmission electron microscopy (TEM)

A drop of SMA/CORM2 (0.05 mg/ml) was applied to a copper grid coated with carbon film and air-dried. The micelle image and the size of SMA/CORM2 micelles were analyzed with a transmission electron microscope (Tecnai F20; FEI, Hillsboro, OR, USA).

2.3.3. Quantification of ruthenium in SMA/CORM2 and determination of CORM2 loading in the micelles

We determined CORM2 loading in SMA/CORM2 micelles by quantifying ruthenium in a sample by use of inductively coupled plasma atomic emission spectrophotometry (ICP-AES). In brief, 10 mg of SMA/CORM2 was dissolved in 50 ml of deionized water, and the solution was then subjected to ICP-AES (ICPS-8100; Shimadzu Corp., Kyoto, Japan), with a detection wavelength at 240.272 nm, to obtain the percentage of ruthenium in the SMA/CORM2 micelles. The CORM2 content was then calculated on the basis of the chemical structure of CORM2.

2.3.4. Release of CO from SMA/CORM2 micelles

SMA/CORM2 was dissolved in different solutions, *i.e.* PBS(−), DMSO, PBS(−) with 0.5% Tween 20, 16.7 mg/ml saponin, 0.5 mg/ml lecithin, buffers of different pH values, or 100% fetal bovine serum (Nichirei Biosciences Inc., Tokyo, Japan), at the micellar concentration of 4 mg/ml (equivalent to 0.4 mg/ml CORM2; 1 ml of each sample). For the DMSO, SMA/CORM2 was first dissolved in PBS(−), which was then diluted 10 times by DMSO to reach the final concentration. In some experiments, free CORM was dissolved in DMSO at 4 mg/ml and 0.1 ml of this solution was added into 0.9 ml of 100% fetal bovine serum to obtain the final concentration of 0.4 mg/ml. The solutions were transferred to 10-ml glass test tubes, which were closed immediately with silicon caps. After scheduled incubation periods at room temperature, 1 ml of the gas in the test tubes was collected *via* a gas-collecting syringe with an 18-gauge needle. Subsequently, the gas was processed by means of a gas chromatograph (TRIlyzer mBA-3000; TAIYO Instruments, Inc., Osaka, Japan) equipped with a semiconductor gas sensor, for CO quantification.

2.4. In vivo pharmacokinetics of SMA/CORM2 and free CORM2

2.4.1. Animals and the DSS-induced murine colitis model

Female ICR mice, 6 weeks old, weighing 20 to 25 g, were obtained from Kyudo Co. (Saga, Japan). All animals were maintained under standard conditions and were fed water and murine chow *ad libitum*. All animal experiments were carried out according to the Guidelines of the Laboratory Protocol of Animal Handling, Sojo University.

We induced murine colitis by giving 2% DSS in drinking water *ad libitum*. Colitis symptoms such as diarrhea appeared after 3 days, and at 7 days, severe symptoms including hematochezia and loss of body weight were observed.

2.4.2. In vivo kinetics of SMA/CORM2 and free CORM2, and the CO concentration in circulation

Normal female 6-week-old BALB/c mice were used in this study. Each mouse received an intravenous (i.v.) injection of 0.1 ml of SMA/CORM2 [20 mg/kg, equivalent to 2 mg/kg CORM2, dissolved in PBS(−)] or free CORM2 (2 mg/kg, dissolved in DMSO) *via* the tail vein. Mice orally receiving SMA/CORM2 (20 mg/kg) were also examined. After scheduled times, mice were killed and blood samples were drawn from the inferior vena cava. To 0.1 ml of blood in a 10-ml glass test tube, 0.4 ml of PBS(−) was added. After purging the tube with nitrogen gas, the nitric oxide (NO) donor NOC7 (10 μl) was added to a final concentration of 1 mM. The glass tube was then closed with a silicon stopper and was incubated at room temperature for 2 h, after which 1 ml of the gas in the test tubes was collected and the CO content was measured by using gas chromatography as described above. CO quantified by this method was believed to be CO that bound to hemoglobin, both the basal CO in circulation and those released from CORM2 or SMA/CORM2, which was purged by NO released from NOC7 because of the higher affinity of NO for hemoglobin compared with CO. After 2 h incubation with NOC7, almost all the CO bound to hemoglobin was liberated (Supplemental Fig. S1).

In some experiments, we used saponin (16.7 mg/ml in 1 N H$_2$SO$_4$) instead of NOC7. Saponin is a compound that is widely used to release CO in blood and tissues [23]. Because of its surfactant property, it disrupts the micellar structure of SMA/CORM2 and facilitates the release of CO. We thus believed that the CO quantified by this method was the total CO in the blood—the CO bound to hemoglobin as well as the CO in SMA/CORM2 or CORM2. We concluded that the difference in the CO in the blood quantified by the saponin method and that quantified by the NOC7 method indicated the CO that was obtained solely from SMA-CORM2 or free CORM2, and we used that value to evaluate the kinetics of SMA/CORM2 and free CORM2 in blood.

2.4.3. Body distribution of SMA/CORM2 and free CORM2

Mice with DSS-induced colitis with symptoms observed at 5–7 days after DSS administration were used in this study. We utilized tissue CO concentrations quantified by means of the saponin method to evaluate the distribution of SMA/CORM2 and free CORM2 and their biological availability, with tissues from mice that had not received any SMA/CORM2 and free CORM2 serving as background tissues. Briefly, at scheduled times after i.v. injections of SMA/CORM2 or free CORM2, mice were killed, blood samples were drawn from the inferior vena cava, and mice were subjected to reperfusion with 20 ml of physiological saline containing heparin (5 U/ml) to remove blood components from the blood vessels of the tissues. Specimens of colon as well as those of normal tissues, including liver, spleen, kidney, heart, and lung, were collected and weighed. PBS(−) at a ratio of 400 μl/100 mg tissue was added to the tubes, followed by homogenization. To 500 μl of homogenized tissue in 10-ml glass test tubes, 200 μl of saponin was added, and the tubes were closed immediately with silicon stoppers. After 20 min of incubation at room temperature, 1 ml of the gas in the test tubes was collected and subjected to gas chromatography as described above.

In some experiments, we used the same protocol with normal 6-week-old female BALB/c mice to investigate the distribution of SMA/CORM2 and free CORM2 in the normal colon.

2.5. In vivo therapeutic effect of SMA/CORM2 in DSS-induced murine colitis

2.5.1. Experimental protocol

Murine colitis was induced by giving DSS orally as described above (Section 2.4.1). SMA/CORM2 dissolved in physiological saline was administered i.v. at 20 mg/kg (0.1 ml, *via* the tail vein) or orally at 40 mg/kg (0.1 ml by using a sonde placed in the stomach) on the 5th day after DSS treatment, when colitis symptoms such as diarrhea appeared (Supplemental Fig. S2). During the experiments, the symptoms and severity of colitis were observed, as described in the next section. On day 7 after DSS treatment when severe symptoms were noted, the mice were killed and blood and colon specimens were collected for biochemical and pathological examinations. Serum samples obtained from the blood were used to determine levels of monocyte chemotactic protein-1 (MCP-1), tumor necrosis factor-α (TNF-α), and interleukin-6 (IL-6), as described below. The length of each colon was measured, and then the colon specimens were fixed with 10% formalin solution and embedded in paraffin. Paraffin-embedded pathological sections (6 μm thick) were prepared as usual for histological examination after hematoxylin and eosin (H&E) staining.

2.5.2. Evaluation of the severity of colitis

We evaluated the severity of colitis by using a semiquantitative disease activity index (DAI), which was determined by scoring changes in the body weight of the animals, presence of occult blood, gross bleeding, and stool consistency, as described in the literature [24]. We used five grades of weight loss (0: either a weight gain or no weight loss; 1: 1–5% loss; 2: 5–10% loss; 3: 10–20% loss; and 4: >20% loss), three grades of stool consistency (0: normal; 2: loose; and 4: diarrhea), and three grades of occult blood (0: negative; 2: occult blood-positive; and 4: gross bleeding). We measured colon length as an indirect marker of inflammation, and we performed pathohistological examinations of colon tissues after H&E staining. Individual mice were graded, and the mean value for each experimental group was obtained.

2.5.3. Effects of SMA/CORM2 on the production of MCP-1, TNF-α, and IL-6 in mice with DSS-induced colitis

We obtained serum samples from mice with DSS-induced colitis as described above, and levels of MCP-1, TNF-α, and IL-6 were quantified by using ELISA kits (Pierce Biotechnology, Inc., Rockford, IL, USA), according to the manufacturer's instructions.

2.6. Statistical analyses

All data are expressed as means ± SD. Data were analyzed by one-way ANOVA followed by the Bonferroni *t*-test. A difference was considered statistically significant when $p < 0.05$.

3. Results and discussion

3.1. Synthesis and physiochemical characterization of SMA/CORM2

SMA/CORM2 was easily prepared by adding CORM2 dissolved in DMSO to the aqueous solution of SMA, after which micelles formed spontaneously *via* non-covalent bonds, similar to our previous results with SMA micelles [22]. The hydrophobic CORM2 formed a hydrophobic core surrounded by styrene residues of SMA, with hydrophobic or other non-covalent interactions, while the hydrophilic maleyl side chain of SMA formed the outer surface facing water (Fig. 1A). The resultant SMA/CORM2 micelles exhibited a single-peak distribution and an apparent hydrodynamic diameter of 165.3 ± 71 nm in aqueous solution, as determined by dynamic light scattering (Fig. 1B). However, TEM

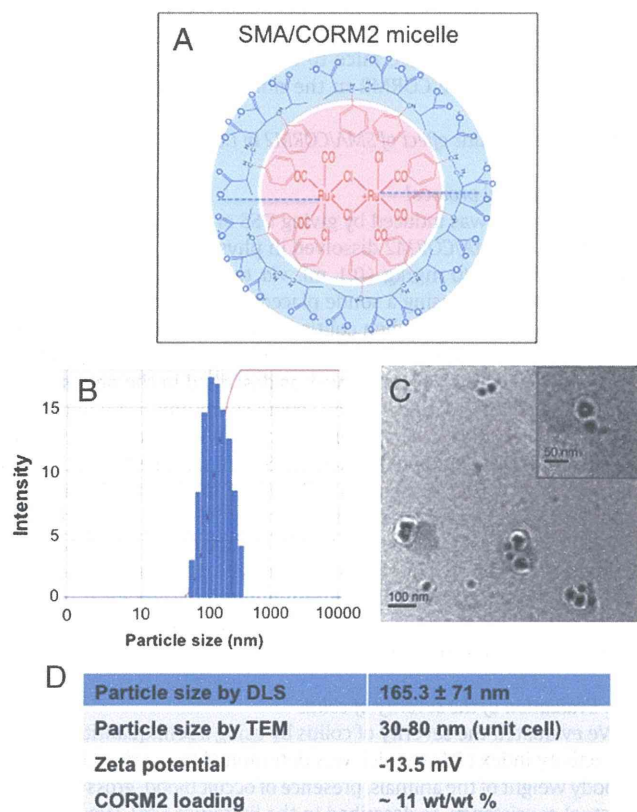|	
Particle size by DLS	**165.3 ± 71 nm**
Particle size by TEM	**30-80 nm (unit cell)**
Zeta potential	**-13.5 mV**
CORM2 loading	**~ 11 wt/wt %**

Fig. 1. Micellar formation and characterization of SMA/CORM2. (A) Diagrammatic illustration of SMA/CORM2 micelle structure. (B) The hydrodynamic size of SMA/CORM2 micelles in aqueous solution determined via dynamic light scattering (DLS). (C) TEM of SMA/CORM2 micelles. (D) Summary of the physiochemical characteristics of SMA/CORM2 micelles. The size as measured by TEM is that of one unit cell of micelles. When 2–4 units are clustered in water, the micelle size agrees well with that found by DLS.

revealed a spherical SMA/CORM2 appearance; most unit micelles had diameters of 30–80 nm, but two or three particles tended to cluster together, and thus the molecules appeared larger, more than 100 nm (Fig. 1C). These findings suggested that SMA/CORM2 self-associated to form supramolecular structures in aqueous medium. In addition, it is interesting that SMA/CORM2 micelles in PBS(−) exhibited a much weaker zeta potential (−13.5 mV) compared with that of free SMA (~−50 mV).

To determine the CORM2 loading in SMA/CORM2 micelles, we performed elemental analysis of the ruthenium (ICP-AES) in CORM2. The content of ruthenium in SMA/COMR2 micelles was 4.1% (w/w) when CORM2 and SMA were applied at the ratio of 1:5 (g/g). CORM2 loading in the micelles was thus calculated to be ~11% according to chemical structure, and the total yield was 66.7% based on CORM2 (Fig. 1D). The resultant SMA/CORM2 showed good water solubility (>50 mg/ml in a physiological water solution). In addition, when the feed ratio of CORM2 to SMA was increased to 1:3, the resultant compounds were difficult to dissolve in water (data not shown), which indicated that high loading of CORM2 may lead to insufficient coverage of the hydrophobic core and thus a reduced water solubility.

3.2. Profiles of CO release from SMA/CORM2

We then used CO-detecting gas chromatography to measure the velocity of CO release from SMA/CORM2 and compared it with that of the parental COMR2. As expected, parental CORM2 in the DMSO solution demonstrated a very rapid CO release rate, i.e. almost all CO was released within 10–30 min (data not shown), whereas SMA/CORM2 in PBS(−) solution manifested a much slower CO release (e.g. <5%/day) (Fig. 2A). Complete release of CO from SMA/CORM2, within 1 h, was

observed for SMA/CORM2 in the DMSO solution (Fig. 2A), because the micelles were completely disrupted in the solvent. These findings indicated the effects of solvents on the stability of the micelles and the CO release properties of SMA/CORM2. Furthermore, when a surfactant (Tween 20 or saponin) was added to an aqueous solution of SMA/CORM2, the micelle structure disintegrated, the surfactant thus facilitating CO release (Fig. 2A). Incubation of SMA/CORM2 in saponin for 24 h resulted in an almost complete release of CO (Fig. 2A), so saponin was used as the CO-releasing agent in our in vivo pharmacokinetic study, as described below. More important, when lecithin, the major component of cell membranes, was added to the SMA/CORM2 solution, CO release was also increased (Fig. 2A), which suggests that SMA/CORM2 micelles may be disrupted during the intracellular uptake process and subsequently release CO. Similar results were observed for other SMA micelles in our laboratory [22,25].

CO release from SMA/CORM2 was also examined at different pH values. As Fig. 2B illustrates, for the range of pH 2 to 10, no significant increase in CO release was found for up to 48 h. This result suggested a pH stability of SMA/CORM2 as well as the possibility of oral administration of SMA/CORM2.

More importantly, we measured the release of CO from SMA/CORM2 in the presence of 100% fetal bovine serum to mimic the in vivo behavior of SMA/CORM2 (Fig. 2C). Compared with free CORM2, which reached a peak CO release in 30 min, SMA/CORM2 had a slower and more sustained CO release, which gradually increased in 24 h and lasted up to 48–72 h. We thus expected that SMA/CORM2 would show superior in vivo pharmacokinetics compared with the parent CORM2, which would guarantee improved bioavailability of CO after systemic administration of SMA/CORM2. We therefore performed a pharmacokinetic study, as described below.

3.3. In vivo pharmacokinetics of SMA/CORM2

We first determined the CO concentration in circulation after i.v. injection of SMA/CORM2 or free CORM2 in normal BALB/c mice. Because most CO exists in circulation as CO-hemoglobin, we used the NO-releasing agent NOC7 to purge hemoglobin-bound CO. Fig. 3A shows that the CO concentration in the blood of healthy BALB/c mice was about 10 nM. Administration of free CORM2 induced a prompt increase in CO (to a 3.5-fold higher value) in circulating blood at 2 h, followed by a decrease in CO because of its removal from the lung through respiration; the CO concentration was about twice that of the basal level after 24 h (Fig. 3A). Similar to the results seen in Fig. 2C, CO in circulation demonstrated a much slower and constant increase after i.v. SMA/CORM2 administration. The CO concentration increased to 3.7 times that of the basal level and was maintained at relatively high levels for up to 48 h (Fig. 3A). In addition, when SMA/CORM2 was administered orally, prolonged high CO concentration in circulation, similar to those after i.v. administration, was also observed (Supplemental Fig. S3A). These findings suggested that superior in vivo bioavailability of CO could be achieved by SMA/CORM2 compared with free CORM2.

We then investigated the in vivo pharmacokinetics of SMA/CORM2 by using saponin to liberate all the CO in circulation, including CO bound to hemoglobin as well as CO from injected SMA/CORM2, as described in Section 2.4.2. We calculated the CO from the SMA/CORM2 that remained in circulation by subtracting hemoglobin-bound CO from total CO quantified by means of the saponin method, and we analyzed the results to evaluate the in vivo pharmacokinetics. As seen in Fig. 3B and Table 1, after i.v. injection SMA/CORM2 exhibited a 35-fold longer blood $t_{1/2}$ (21.2 h) compared with free CORM2 (0.6 h). Moreover, the area under the concentration vs. time curve of SMA/CORM2 was about 17 times greater than that of free CORM2, and the body clearance of SMA/CORM2 was about 16 times slower than that of free CORM2 (Table 1).

In addition, when administered orally, blood concentration of SMA/CORM2 continuously increased to 2 h after which it gradually